THE INFLUENCE OF CRACK CLOSURE ON THE FATIGUE CRACK PROPAGATION IN THE ALUMINIUM ALLOY AL MG SI 1

R. Scheffel and K. Detert*

The fatigue crack propagation behaviour of the aluminium alloy AlMgSi 1 has been examined in the under- and over-aged conditions for one load ratio R=.1 and in the under-aged condition for load ratios between 0,1 and 0,6.
The results have been compared with those of the well examined alloy AlZnMgCu1,5. The crack growth rates in AlMgSi1 for given cyclic stress intensity and load ratio were found to be much smaller than those in AlZnMgCu 1,5.
These results can be explained by crack closure which was observed to occur in AlMgSi1 but could not be detected in AlZnMgCu1,5. The dependence of growth rates on the cyclic stress intensity range is however very similar if the applied stress intensity range is replaced by the effective one.

INTRODUCTION

Among the aluminium alloys the age hardened alloys of the type AlZnMgCu (AA 7075) have been the object of many investigations as a result of their outstanding technological importance. The alloys of the type AlMgSi were only to a minor degree subject of similar efforts to study their mechanical behaviour on a broader base. Particular attention concerning AlMgSi alloys has been attached to the influence of the grain size and the different kinds of precipitated particles on the mechanical properties of the aged alloys (1)-(3). In recent years the interest is focussed on fatigue crack initiation and propagation behaviour:

Alloys with coarse grains show lower crack propagation rates at a given cyclic stress intensity whereas those with fine grains have a longer crack initiation period. Thus a combination of fine grains on the surface and coarse grains in the bulk exibit best fatigue lives (4).

Alloys with increasing volume fractions on Mn-bearing dispersoids (alpha - $Al_{12}Mn_3Si$ particles of approximately 0,1 µm diameter) show a decrease in the fatigue crack growth rate due to a decrease in the degree of intergranular fracture caused by the homogenization of slip by dispersoid particles (5). A particle fracture of the dispersoid phase seldom occurs, even

*Universität Gesamthochschule Siegen, Institut für Werkstofftechnik, Paul-Bonatz-Straße 9-11, 5900 Siegen, Germany

in regions of high matrix strain. This observation can be explained by the roughly equiaxed shape of the dispersoid phase (6). The more plate-like particles of the Cr-bearing phase present in the alloys of the AlZnMgCu type were observed to fracture ahead of the crack tip and thus accelerated the fatigue crack propagation rate (7).

The present study was undertaken with an AlMgSi1 alloy, commercially manufactured, in order to investigate plasticity effects during cycling which are known to occur at the crack tip. These effects are studied at different crack lengths in order to determine their influence on fatigue crack propagation.

EXPERIMENTAL MATERIALS AND METHODS

The composition and the grain size of the AlMgSi alloy used is compiled in Tab. 1. The alloy was industrially DC cast, extruded to bars and then rolled to slabs of 1000 mm x 700 mm x 25 mm. Pieces of 130 mm x 130 mm x 25 mm were cut out, solution treated at 540°C/60 min and aged to a hardness of ca. 100 HB 2.5/62,5. The aging time was 3 h for the underaged and 2 d for the overaged conditions. The tensile properties are given in Tab. 2. The CT-specimens (W=0,1 m, B=0,015 m) were finally machined with the crack in the LT orientation according to ASTM specification E647-78T.

The fatigue crack propagation tests were performed on a closed-loop servo-hydraulic testing machine under load controlled sinusodial tension tension testing at a frequency of 20 Hz. Two test series were performed:

1. Underaged and overaged specimens were cycled under a constant stress ratio R=0,1. The crack was initiated at a cyclic stress intensity $\Delta K > 12$ MPa$\sqrt{m}$, eg the applied maximum load was 16 kN. A stepwise load decrease of less than 20% per step at constant R was applied after the fatigue crack had left the Chevron notch. At the beginning of the actual rements the cyclic stress intensity was again ca. 12 MPa$\sqrt{m}$.

2. Underaged specimens were cycled under different stress ratios R=0,1, 0,2, 0,4 and 0,6, but the maximum load in each cycle was fixed at 10 kN.

Fatigue crack growth was investigated by means of two methods:

a) Crack lengths were measured optically with a mobile microscope and the specimen was illuminated by stroboscopic light. The specimens were electrolytically polished along the expected crack path and marker lines were engraved each millimeter. This preparation allowed an accuracy of measurement of 0.02 mm and also microscopic investigation of details of the crack propagation process at the specimens surface.

b) Compliance measurements were performed with clip gauges which had been fixed between two knives at the crack mouth. The signals for load and crack opening displacement during selected cycles were registered with a transient recorder and plotted as a curve on a X-Y-plotter. Tne compliance could be determined from the slope.

RESULTS

Crack propagation curves

The experimental data were evaluated according to ASTM E 647 - 78T specifications: Numerical differentiation of the measured crack length a as a function of the number of cycles N gave the crack propagation rate da/dN. The cyclic stress intensity ΔK was calculated using

$$\Delta K = \frac{\Delta P}{B\sqrt{W}} f\left(\frac{a}{W}\right) \qquad (1)$$

$$f\left(\frac{a}{W}\right) = \frac{2+\frac{a}{W}}{\left(1-\frac{a}{W}\right)^{3/2}} \left(0.886+4.64\frac{a}{W} - 13.32\left(\frac{a}{W}\right)^2+14.72\left(\frac{a}{W}\right)^3 - 5.6\left(\frac{a}{W}\right)^4\right) \qquad (2)$$

ΔP is the load range between maximum and minimum load, B (=15 mm) the specimen's thickness and W (=100 mm) the characteristic dimension.

The crack propagation curves for R = 0.1 in Fig. 1 are as usually presented in log - log coordinates. The curves can be fitted (in the medium range of ΔK) by an empirical power function:

$$\frac{da}{dN} = \alpha^* \left(\frac{\Delta K}{\Delta K^*}\right)^n \qquad \alpha^* = 1\mu m/cycle \qquad (3)$$

In the log - log plot this function corresponds to a straight line with the slope n running through the point (ΔK^*, α^*).
The mean values are ΔK = 17,7 MPa$\sqrt{m}$, n = 4,9 for age hardened and ΔK = 16,1 MPa$\sqrt{m}$, n = 4,0 for overaged specimens in Fig. 1.

As Fig. 2 shows for the age hardened specimens these parameters depend on the stress ratio R: An increase of the mean stress shifts the curves to the left, eg. to lower ΔK values and additionally leads always to a smaller exponent n of the Paris low.

Compliance

An example of the plot of load P vs crack opening displacement v for AlMgSi1 is given in Fig. 3a. The curves are composed of two straight line pieces connected by a very small transition range. The slope of the lower parts (eg. the specimens compliance) seems to be independent of the actual crack length and thus only seems to represent the depth and geometry of the starter notch. At low loads the crack seems to have 'dissappeared'. This item is an essential one for the understanding of the crack propagation curves and will be discussed in later.

The slope at higher loads depends strongly on the crack length and leads to the usual normalized compliance (CEB) values (after transformation of the crack opening displacement v with respect to the load line) and are identical with those values given in the literature (8).

A measure for the transition between the two straight lines is the load at the intersection. This load decreases with increasing crack length. However inserting this load and the corresponding crack length into equations like Eqs. 1,2 one yields a practically costant 'crack opening stress intensity' for each single crack propagation curve. The mean value is:

$K_{op} = 9 \pm 1.9$ MPa$\sqrt{m}$

DISCUSSION

Fig. 1 shows that the fatigue crack propagation rate seems to be slightly lower in the underaged specimens than in the overaged. But since the scatterbands overlap, a clear decision cannot be made now. The fatigue crack growth rates agree with those for alloys of similar composition and grain size given in the literature (4,5) (Tab. 1), but the difference to AlZnMgCul,5 is surprisingly large as can be seen in Fig. 4. (The composition and heat treatment of the latter alloy are compiled in Tab. 3).

From the unusual shape of the load vs. crack opening displacement curves with two slopes in Fig. 3a one must conclude that an extraordinary strong crack closure effect has to be taken into account for the present AlMgSi alloy: in order to separate the two crack surfaces from each other during loading a certain force must be applied. For the sample in Fig. 3a this load corresponds to a stress intensity of about K_{op} = 11 MPa$\sqrt{m}$. Only above this value the crack tip 'feels' the load changes as stress intensity changes. Thus plastical deformation at the crack tip should occur to a large extent only as long as the stress intensity changes between K_{op} and K_{max} (the maximum stress intensity). If this interpretation is true it should be physically more significant to plot da/dN as a function of $\Delta K_{eff} = K_{max} - K_{op}$ instead of $\Delta K = K_{max} - K_{min}$. Fig. 5 supports this interpretation: It shows that even the crack propagation curves for different R values taken from Fig. 2 coincide in a medium range of ΔK_{eff} whereas they did not in the original ΔK presentation. Furthermore good agreement between AlMgSi1 (ΔK_{eff} on the abcissa) and AlZnMgCul,5 (ΔK on the abcissa) is obtained as Fig. 5 demonstrates. The load vs. crack opening displacement curves of the latter alloy are ideal straight lines (Fig. 3b), which means, that there is no difference between ΔK_{eff} and the nominal ΔK.

The fatigue crack growth data in Fig. 1 can be fitted by a Paris law giving an exponent of approximately 4 which lies in the middle of the range 2 <n< 10 reported in the literature. This value of the exponent might however be misinterpreted (if crack closure is disregarded) as indicating that a damage accumulation model might be suitable to explain the fatigue crack propagation data of AlMgSil. Taking correctly into account that crack closure happens the fatigue crack growth rate da/dN should be plotted versus ΔK_{eff} and then the Paris fit should be made. Fig. 5 shows that then an exponent of 2 is obtained indicating that in a limited range of ΔK_{eff} the fatigue crack growth rate is controlled by the reversed crack opening displacement (9). If ΔK_{eff} is normalized with respect to the elastic modulus (E = 70000 MPa) one obtains the crack propagation formular

$$\frac{da}{dN} = C \left(\frac{\Delta K_{eff}}{E}\right)^2 \qquad (4)$$

with the dimensionless constant c = 8,2 (a similar result for steels is given in (17)). A deviation from the straight line in Fig. 5 occurs when K_{max} becomes becomes greater than 21.5 MPa$\sqrt{m}$ and at a crack propagation rate of 1000 µm a nearly constant K_{max} of about 30 MPa$\sqrt{m}$ is found. Both features indicate that the crack propagation mechanism changes to a K_{max} controlled one.

There are mainly three mechanisms suggested in the literature which ar used to explain crack closure (10).

1. Plasticity-induced crack closure first discussed by Elber (11, 12). This mechanism should be dominant in the plain stress condition (13 14).
2. Oxide-induced crack closure at near threshold crack growth and low ratios (eg. at plain strain conditions).
3. Roughness induced crack closure, which can arise from an irregular rough fracture surface morphology (15, 16).

Evidence has been found, that the latter two mechanisms are active.

SYMBOLS

a	= crack length (m)
da/dN	= crack growth rate (µm/cycle)
a_0	= constant 0.1 µm/cycle
B	= CT specimen thickness (m)
c	= 8,2 = dimensionless constant
E	= elastic modulus (MPa)
K_{max}	= maximum stress intensity (MPa$\sqrt{m}$)
K_{min}	= minimum stress intensity (MPa$\sqrt{m}$)
K_{op}	= crack opening stress intensity (MPa$\sqrt{m}$)
ΔK	= applied cyclic stress intensity (MPa$\sqrt{m}$)
ΔK_{eff}	= effective cyclic stress intensity (MPa$\sqrt{m}$)
ΔK^*	= adjustable constant (MPa$\sqrt{m}$)
n	= crack growth exponent
N	= number of cycles
P	= applied load (N)
ΔP	= applied load range (N)
R	= K_{min}/K_{max} = stress ratio
W	= CT specimen width according ASTM specification E647-78T (m)

REFERENCES

1. Scharf, G. and Grezemba, B., Aluminium, 58, (1982), 391
2. Schwellinger, P., Aluminium, 55, (1979) 136
3. Dunwoody, B. J., et al, Inst. of Metals, 101 , (1973) 172
4. Ruch, W. and Gerold, V., Proc. 4th ECF, Leoben, Austria , (1982), 383
5. Edwards, L. and Martin, L.W., Proc. 5th ICF, Cannes, France , (1981), 323
6. Dowling, J.M. and Martin, J.W., Proc. 4th ICF, Waterloo, Canada (1977), 87
7. Albrecht, J., et al, Proc. 4th Int. Conf. on Strength of Metals and Alloys, Nancy, France, (1982), 463
8. Marci, G. and Bazant, E., Zeitschrift für Werkstofftechnik, 8, (1977), 235
9. Garrett, G.G. and Knott, J.F., Metall. Trans. A, 7a, (1976). 884
10. Richie, R.O. and Suresh, S., Metall. Trans., 13a, (1982), 937
11. Elber, W., Eng. Fracture Mechanics 2, (1970) 37
12. Elber, W., ASTM STP 486, (1971) 230
13. Marci, G. and Packman, P.F., Zeitschrift für Metallkunde, 68, (1977) 47
14. Lindley, T.C. and Richards, C.E., Mater. Science and Engineering, 14, (1974) 281
15. Walker, N. and Beevers, C.J., Fatigue of Eng. Materials and Structures, 1, (1979) 135
16. Ritchie, R.O., Proc. 1st Intern. Conf. in Fatigue Thresholds, Stockholm, Sweden , (1981)
17. Hahn, G.T. et al, AF 336-70-C-1630, Batelle Memorial Inst., Columbus, Ohio, 1971

Tab. 1: Composition of the investigated alloys (weight%)

	present work AlMgSi1	Edwards, Martin (5) MH	Ruch, Gerold (4) AlMgSi1
Si	1.05	1,03	1,00
Fe	0,21	0,001	0,40
Mn	0,70	0,60	0,80
Mg	1,02	0,61	1,00
Cu	0,01		
Zn	0,01		
grain size in µm	100-300	80	320-450 (cc) 5- 15 (cf)subgrains

Tab. 2: Tensile Properties

heat-treatm.	$R_{po,2}$ MPa	R_m MPa	E MPa	true fracture stress MPa	A_5 %	Z %	hardness HB(2,5/62,5)
over-	282	312	70235	392	11,4	34,4	97
aged	248	294	68454	410	13,6	36	96
(oa)	286	313	68898	399	10,8	34,4	99,5
under-	250	294	69766	418	13,6	37,6	99,5
aged	261	284	70735	398	11,0	37,6	99,5
(ua)	248	293	70539	408	13,4	36	99,5

Tab. 3: Heat treatment, mechanical properties and chemical composition of the AlZnMgCu1,5 alloy

a) solution treatment: 470°C/30 min (saltbath)
b) plastically strained: 1,5%
c) aging treatment: 1st step 120°C/12 h
2nd step 170°C/5,5 h (saltbath)

$R_{po,2}$ MPa	R_m MPa	A_5 %	hardness HB (2,5/62,5)
527	578	8,8	164
526	576	9	164

Cu	Fe	Mg	Mn	Si	Zn	Ti	Cr
			weight %				
1,42	0,20	2,52	0,10	0,14	5,90	0,04	0,20

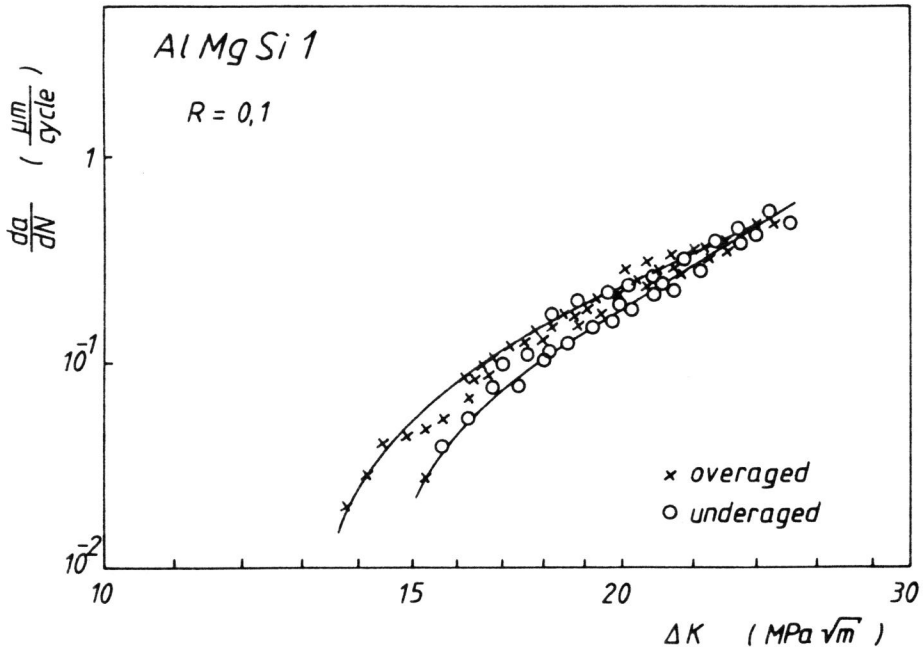

Fig. 1 Influence of the aging treatment on Crack Propagation

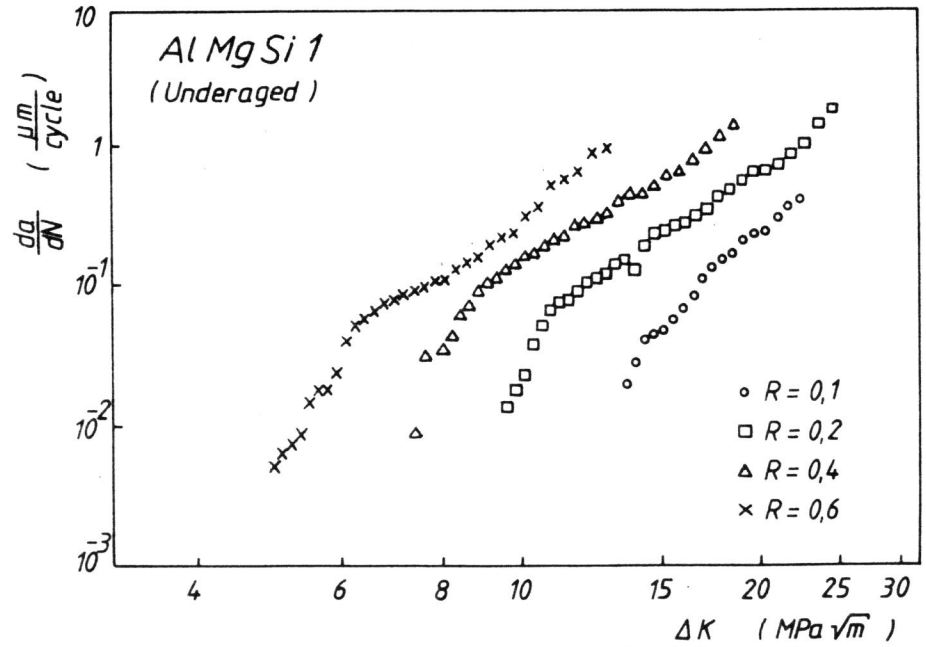

Fig. 2 Influence of the stress ratio on Crack Propagation

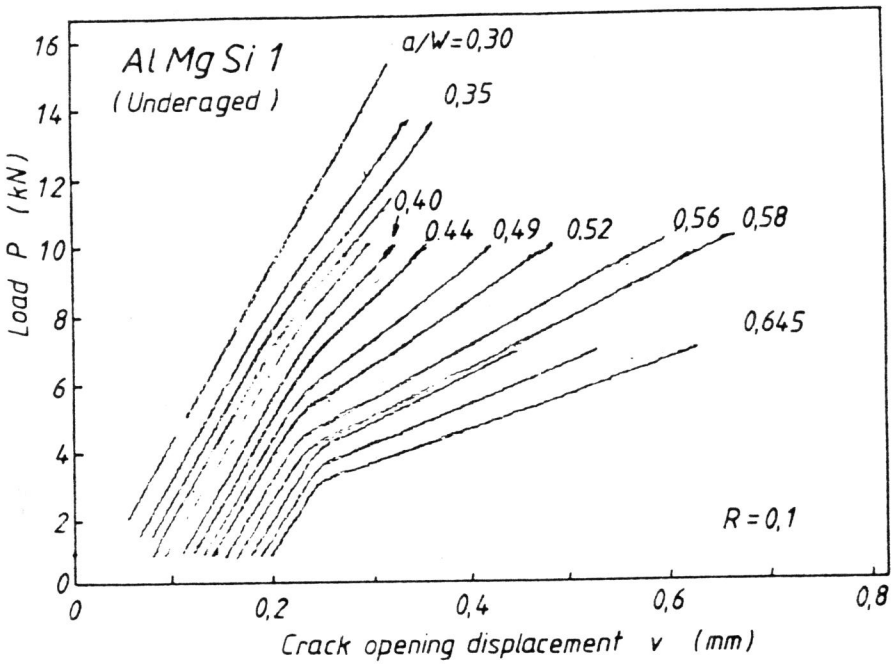

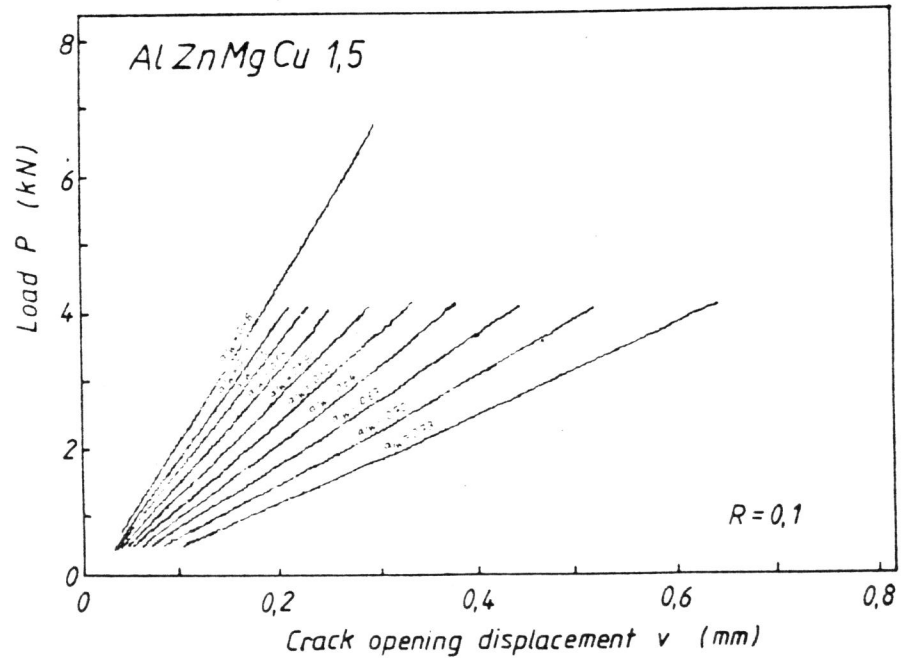

Fig. 3 Plots of Load versus Crack opening displacement for

a) AlMgSil (underaged)
b) AlZnMgCul,5 (see Tab.3)

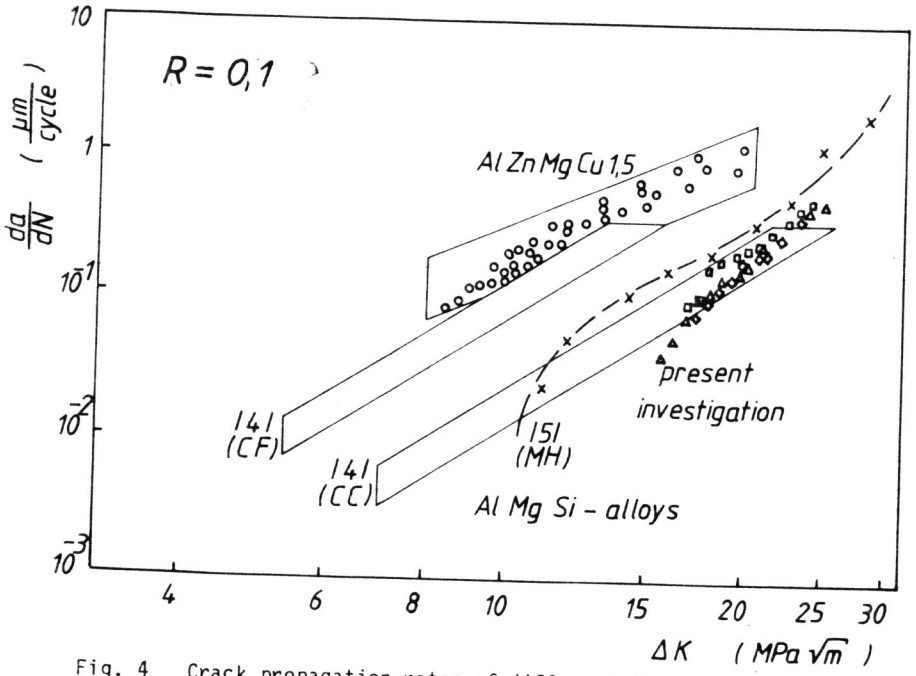

Fig. 4 Crack propagation rates of different AlMgSi alloys compared with AlZnMgCul,5.

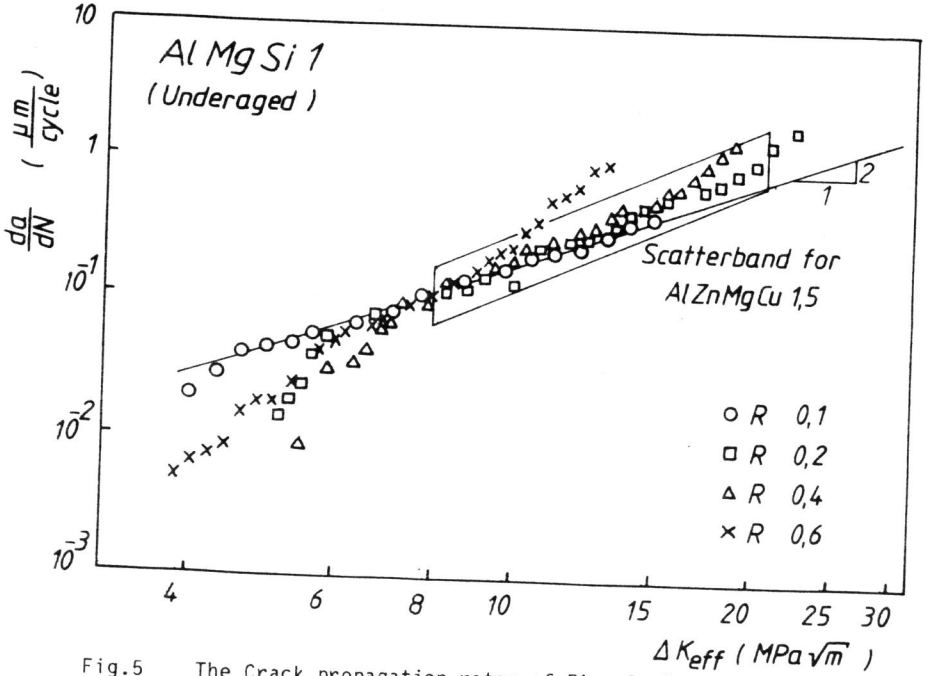

Fig.5 The Crack propagation rates of Fig. 2 plotted as a function of the effective cyclic stress intensity from Fig. 2 (in comparison the crack propagation rate of AlZnMgCul,5 from Fig. 4)

LIFE ASSESSMENT OF 316 L STAINLESS STEEL AT 600 °C UNDER SUCCESSIVE LOADING BY FATIGUE AND CREEP.

R. ROUX, J. CHARRIER, C. GASC*

Successive loading by fatigue and creep,or inversely, has revealed some specific aspects of damage accumulation in the material. The general study of that problem is particularly complex in the case of 316 L stainless steel, because of the anisotropy of plastic deformation, the existence of aging at 600 °C and the memory effect of successive stress levels.

These reasons, added to the scatter of fatigue and creep test results, make difficult the interpretation of damage accumulation results. But quantitative analysis of fracture surfaces appearence has enabled the separation of the effects of initial creep upon fatigue crack initiation, propagation, and final fractures.

INTRODUCTION

For some years, the combined effect of high temperature loading in fatigue and creep is the object of many studies. Indeed, the materials used at elevated temperature are subjected to important thermal stresses and strains, due to the non-homogeneous temperatures in the structure. These effects can be very important in austenitic stainless steels whose thermal conductivity is small (strong temperature gradients) and dilatation coefficient is high (strong strain gradients).

Generally, these phenomena are studied by low-cycle fatigue tests at constant temperature with a hold times at the top or/and at the bottom of each cycle. So one obtains the superposed effects of imposed strain fatigue, and of relaxation during each hold time. For different hold times, from a few seconds to about ten minutes, one can study the connecting mechanisms between these two processes, and their effects on the damage and on the life of specimens.

Conversely, in this study, we have applied, one after the other, a fatigue loading during a fraction of estimated life, and then a creep loading at constant stress up to the fracture, or inversely. The aim was the estimation of damage accumulation of the two successive loadings in different situations, because the microscopic and macroscopic damage created by the first loading modifies the behaviour and the life during the second loading.

* Laboratoire de Mécanique et Physique des Matériaux
E.R.A. 123 du C.N.R.S.
GRECO Grandes Déformations et Endommagement
E.N.S.I.M.A., 86034 POITIERS , FRANCE.